31st EPS Conference on Plasma Phys. London, 28 June - 2 July 2004 ECA Vol.28G, P-4.195 (2004)

Observation of CAEs on MAST

L.C.Appel[1] , R.J. Akers[1] , T. Fülöp[2] , R.Martin[1] , and T.Pinfold[1] .
[1] *EURATOM/UKAEA Fusion Association, Culham Science Centre, Abingdon, Oxon, OX14 3DB.* [2] *Department of Electromagnetics, Chalmers University of Technology, and Euratom-VR Association, Göteborg, Sweden.*

1 Introduction

Quasi steady-state high frequency magnetic fluctuations have been observed on MAST well above frequencies where Toroidal and Elliptic Alfvén eigenmode (TAE and EAE) activity was previously reported [1]. In this paper we present evidence to support the view that these modes are examples of Compressional Alfvén Eigenmodes (CAEs), and have similarities to high-frequency activity reported on NSTX [2]. In the following section we provide more details on the observation of magnetic fluctuations. Section 3 describes calculations of the Neutral Beam (NBI) fast particle drive. Section 4 describe comparisons with theoretical predictions of CAE mode frequencies and growth rates.

2 Observations of high frequency activity

Fig 1 shows an example of high frequency activity from MAST discharge 9429. Compared to observations of TAEs and EAEs seen on MAST, the activity is extremely long-lived and consists of multiple discrete modes occurring simultaneously in two frequency bands. Over the duration of the activity, there is a large upward drift in frequency. Within each band the toroidal mode numbers identified are sequential in n with frequency separation 15kHz. The frequency separation of modes with equal n occurring in the two bands is 170kHz. Following each sawtooth crash, the activity ceases temporarily, probably due to a reduction in the fast-particle drive. When the activity resumes, the mode numbers remain unchanged, but there is a small jump (decrease) in the mode frequencies.

The observations of high-frequency activity are obtained from the OMAHA magnetic diagnostic. During this experimental campaign the Nyquist frequency was $f_{nyq} = 1$MHz; the cut-off frequency was effectively limited by the first self-resonance of the Mirnov coils (≈ 7MHz).

The magnetic activity shown in Fig 1 occurred in at least ten other discharges during the MAST electron Bernstein wave heating (EBWH) campaign in June 2003. As the high-frequency activity was observed both with and without ECRH heating the influence of ECRH on the modes was concluded to be insignificant. For the purpose of EBWH, the feature of these discharges is a steep edge density gradient; this is also a requirement for the occurrence of CAE modes [3]. Another feature of these discharges is a flattening of $|B|$ outboard of the magnetic axis. In all discharges a 1.5MW 47keV co-injected deuterium beam (i.e. in the direction of I_p and counter to the toroidal field) was used to heat a deuterium plasma beginning from $t = 100$ms. At the onset of high frequency activity (always after t=200ms), the plasma current had reached a steady state value of 750kA, with toroidal beta $\beta_t \approx 6\%$, and there were regular ELMS and sawteeth. The toroidal mode numbers indicated in Fig 1 were obtained by the method described in [4]. The confidence (or accuracy) of these mode numbers is expressed as the probability that random noise could generate the same result (i.e. a low figure is desirable); for the central modes in each group, the confidence is $< 10\%$, whereas for the smaller amplitude components, the confidence is $\leq 20\%$. In practice, the same result obtained at many times suggests that these confidence levels are unduly pessimistic.

As stated in Fig 1, the data contained in the spectrogram is likely to be aliased in frequency. Transforming the frequencies using $f \rightarrow 2hf_{\rm nyq} - f$ where h is an integer leads to the following consequences.

- the rotation direction of modes and NB-heated particles is the same.
- The Alfvén velocity (v_A) and mode frequency both increase during 200ms<t<280ms.
- The sudden increase in mode frequency following each sawtooth crash is explained by a step increase in v_A due to a decrease in density at the resonant surface.

For the purposes of analysis, this paper will concentrate on discharge 9429 at time 280ms due to the availability of a high resolution (300-point) measurement of electron density and temperature. At that time, the ion cyclotron frequency ω_c, and v_A both on the mid-plane take the values $\omega_c(R_{mag})$=3.8MHz, and $v_A(R_{mag})$=9.7×10^5m/s, respectively; also the velocity of the injection energy of the NBI is in the range $2 < v_{beam}/v_A < 3$, and the non-thermal ion energy content is 8kJ. For 200ms< t <280ms, the mode frequency and $v_A(R_{mag})$ increases by $\Delta f = 250$kHz and $\Delta v_A(R_{mag}) = 10^5$m/s respectively.

3 Energetic particle distribution

The NBI Fokker-Planck code LOCUST was run on discharge 9429 at t=280ms to obtain the distribution of energetic ions. The results from LOCUST were mapped to the constant of motion (COM) space (p_ζ,E,μ; σ) where p_ζ, E, μ and σ are the toroidal canonical momentum, energy, first adiabatic invariant, and the sign of $v_\parallel/v$ respectively. The method, described in [1], showed that in general the mapping from physical coordinates to COM-space is not unique, and care needs to be taken to include the resonant part of the distribution.

Overall the tail-distribution comprises ions in the following proportions: counter-passing (12%), co-passing, confined within separatrix (40%), co-passing, crossing separatrix (8%), and trapped (40%). Detailed analysis reveals a bump-on-tail in $f(E)$ for the co-passing population as shown in Figs 2 and 3 with the density peaking at the stagnation orbits. A similar phenomenon is observed in $f(\mu)$ for the counter-passing population. Finally, Fig 4 shows a localised bump-on-tail in $f(\mu)$ for co-passing orbits near the plasma edge at the NB injection energies.

4 Calculation of eigenmodes

Calculations have been carried out based on discharge 9429 at t=280ms using the theory of Smith *et al.* [5]. The theory takes into account finite toroidicity and ellipticity in the limit $\omega \sim \omega_c$ and $k_\parallel \ll k_\perp$. The radial structure is approximately described by the 1-D Schrödinger wave equation [3, 2, 5] $(\nabla_r^2 - V(r))\hat{B}(r) = 0$ where $V(r) \approx (m/\kappa r)^2 - (\omega/v_A)^2$. Competition between the two terms can lead to a potential well and the existence of eigenmodes localised at the outboard edge of the plasma. The approach uses a ballooning representation for the poloidal dependence. Retaining only the lowest order term, solutions are sought in the form $X(\rho,\nu) = X_0 h_s[(\rho-\rho_0)/\Delta]h_p[\nu/\eta]\exp(inq(\rho)\nu)$ where $h_s(x) = H_s(x)\exp(-x^2/2)$ in which $H_s(x)$ is the Hermite polynomial of degree s. In this expression, ρ is a radial coordinate, ν is the modified poloidal angle, ρ_0 is the radial localisation of the mode, Δ is the radial mode width, and η is the poloidal width. The results for a given n, s and p always yield two modes, one well localised in radial extent and the other well localised in in poloidal extent. For the case, n=7, s=0, p=0 the solutions are: (i) ρ_0=37cm, Δ=12cm, η =0.33,

$\omega = 2\pi \times 1.74 \times 10^6$rad/s (ii) ρ_0=35cm, Δ=4.8cm, η=1.64, $\omega = 2\pi \times 2.156 \times 10^6$rad/s. The first solution agrees well with the alias-corrected measured frequencies taking $h = 1$ (i.e. measured frequencies of the two bands transform to 1.7MHz and 1.5MHz). The remaining calculations are for the solution with the smaller eigenvalue. An estimate of the frequency difference between adjacent poloidal harmonics is obtained by computing the frequency for p=1 and yields $\delta f_p = 154$kHz. This compares favourably with the measured frequency difference of the two bands (170kHz). However, the computed frequency difference between adjacent toroidal harmonics is δf_n=213kHz which is significantly larger than the measured frequency difference. This discrepancy cannot easily be accounted for. Finally, the change in mode frequency resulting from applying a fixed scaling to the density profile yields (for $n = 8$) $\Delta f/\Delta v_A$=2.49m^{-1} remarkably close to the experimentally measured value (=2.5m^{-1}).

The calculation of linear growth rates, based on equation 50 of [3] with $E_\theta \gg E_r$ in the limit $\omega < \omega_c$, predicts that all the candidate modes are stable. However, boosting $f(E, p_\zeta, \mu; \sigma)$ by a factor of 5 when $\partial f/\partial E > 0$ or $\partial f/\partial \mu > 0$ (i.e. amplifying the bump-on-tail) results in instability driven by the $l = 1$ resonance. Considering the limitations of this theory (it is strictly valid only at low toroidicity), it is reasonable to conclude that the modes may be close to marginal stability.

5 Conclusions

High frequency activity well above the TAE/EAE frequency range has been observed on MAST. The data is likely to be aliased in frequency, and theoretical calculations provide strong evidence that the actual mode frequencies are around 1.5 to 1.7MHz. Theoretical calculations predict that the measured mode activity is well localised to the outboard mid-plane with a frequency (for n=7) close to the measured value. The frequency difference of the two bands is accounted for well. However, the fine-scale splitting due to different toroidal mode numbers is poorly reproduced by the theory. Analysis of the fast-ion distribution function in COM-space reveals a bump-on-tail in $f(E)$ and $f(\mu)$ due to density accumulation at the stagnation orbits. Calculations of wave drive indicate that the modes become unstable if the drive gradients are boosted by a factor of 5. Considering that the theory is strictly applicable to low toroidicity, the result is taken as indication that the modes may be close to marginal stability.

Future theoretical work will concentrate on improving the calculation of the eigenmodes (for example by including the flattening of $|B|$ close to the resonance location), thereby improving the calculation of the finite-scale frequency splitting. In addition further measurements of CAEs are planned with higher digitisation rates.

Acknowledgements: This work was jointly funded by the UK Engineering and Physical Sciences Research Council and EURATOM.

References:

[1] L. C. Appel *et al.*, in *Proceedings of the Joint Lausanne-Varenna International Workshop on Theory of Fusion Plasmas and Varenna* (Società Italiana di Fisica, Via Saragozza 12, 40123 Bologna, Italy, 2002).

[2] N. Gorelenkov *et al.*, Nucl. Fusion (2002).

[3] N. Gorelenkov and C. Cheng, Phys. of Plasmas (1995).

[4] M. J. Hole and L. C. Appel, in *Contributions to the 30th EPS Conference on Controlled Fusion and Plasma Physics 7-11 July 2003, St Peterburg, Russia* (European Physical Society, Europhysics Letters, 27 Rue de la Vendée, POB 69, CH-1213 Petit Lancy 2, 2003), Vol. P-3, p. 132.

[5] H. Smith, T. Fülöp, M. Lisak, and D. Anderson, Phys. of Plasmas (2003).

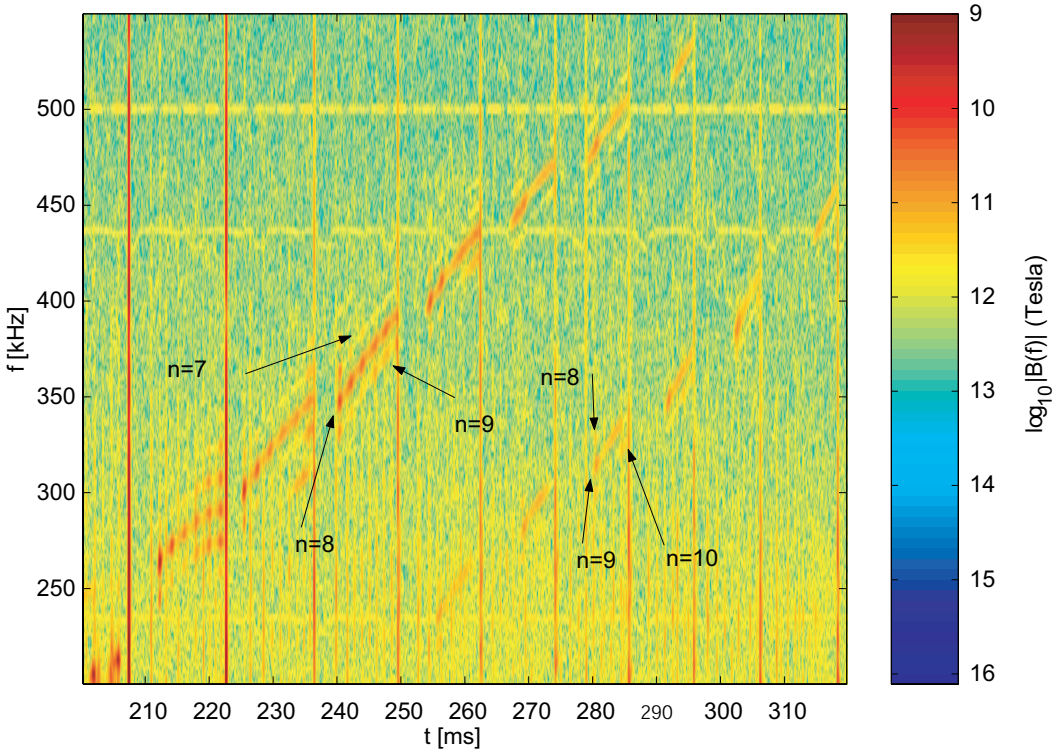

Figure 1: *Spectrogram of magnetic fluctuations showing evidence of discrete high frequency modes. The magnitude of the fluctuations at the Mirnov coils is approximately* $10^{-10}\,T$. *It is important to note that the data is likely to be aliased in frequency.*

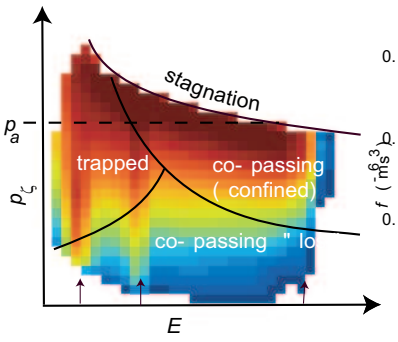

Figure 2: *Variation of* $f(p_\zeta, E, \mu; \sigma)$ *for a co-passing population at constant* μ. *The NB injection energies are indicated by arrows.*

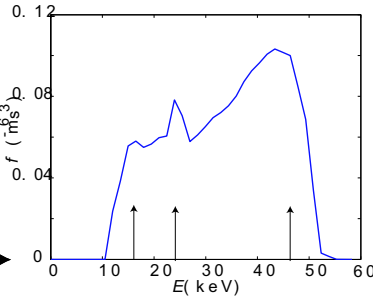

Figure 3: *Illustration of a bump-on-tail in f(E) for a co-passing population with* $p_\zeta = p_a$ *and using the same value of* μ *as in Fig 2. The arrows indicate the principal injection energies of the NBI.*

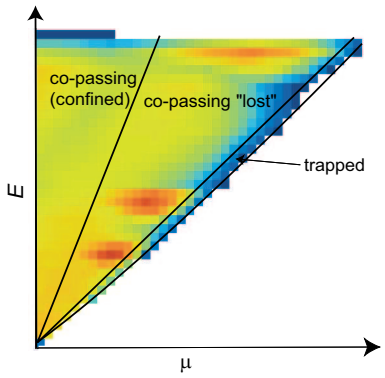

Figure 4: *Variation of* $f(p_\zeta, E, \mu; \sigma)$ *for a co-passing population at constant* p_ζ. *The density is locally increased at the injection energies of the NBI.*